

543 (1968).

³E. Uggerhøj and F. Frandsen, Phys. Rev. B 2, 582 (1970).⁴R. Behnisch, F. Bell, and R. Sizmann, Phys. Status Solidi 33, 375 (1969).⁵R. L. Walker, B. L. Berman, R. C. Der, T. M. Kavanagh, and J. Khan, Phys. Rev. Letters 25, 5 (1970).⁶F. Frandsen and E. Uggerhøj (unpublished).⁷W. M. Gibson, J. B. Rasmussen, P. Ambrosius-Olesen, and C. J. Andreen, Can. J. Phys. 46 551 (1968); L. Chadderton and M. Andersen, Thin Films 1, 229 (1969).⁸P. Lervig, J. Lindhard, and V. Nielsen, Nucl. Phys. A96, 481 (1967).⁹J. U. Andersen, Kgl. Danske Videnskab. Selskab,Mat.-Fys. Medd. 36, No. 7 (1967).¹⁰S. T. Picraux, J. A. Davies, L. Eriksson, N. G. E. Johansson, and J. W. Mayer, Phys. Rev. 180, 873 (1969).¹¹J. U. Andersen and E. Uggerhøj, Can. J. Phys. 46, 517 (1968).¹²R. E. DeWames and W. F. Hall, Acta Cryst. A24, 206 (1968).¹³P. B. Hirsch, A. Howie, R. B. Nicholson, D. W. Pashley, and M. J. Whelan, *Electron Microscopy of Thin Crystal* (Butterworths, London, 1965).¹⁴C. R. Hall, Proc. Roy. Soc. (London) A295, 140 (1966).¹⁵J. Lindhard, Kgl. Danske Videnskab. Selskab, Mat.-Fys. Medd. 34, No. 14 (1965).

PHYSICAL REVIEW B

VOLUME 3, NUMBER 3

1 FEBRUARY 1971

Covalency Effects on the 3d-Charge-Density Distribution in Solid Ferrous Compounds

Y. Hazony

Department of Chemical Engineering, Princeton University, Princeton, New Jersey 08540

(Received 18 June 1970)

A phenomenological description of the 3d-charge-density distribution in solids, based on Mössbauer hyperfine interaction data, studies of crystal structures, EPR, neutron scattering and optical spectroscopy, has been developed for divalent iron ions in solids. From this work, it appears that one can obtain an internally consistent picture of the 3d-charge-density distribution in solids by allowing for large, but distinctly different, modifications of the radial 3d(e_g) and 3d(t_{2g}) electronic wave functions. These modifications vary continuously with covalency on going from the completely ionic to the completely covalent ferrous compounds. They account for the large changes (in order of magnitude) in the mean 3d charge (or spin) densities, indicated by the experimental data. These results cannot be explained by theoretical models of bonding based on crystal field and molecular-orbital theories, using *free-ion* wave functions. The present model emphasizes the importance of the radial modifications of the 3d wave functions, thus supporting the point of view that, in self-consistent-field-type theoretical computations, the radial wave functions should be described by variational rather than fixed parameters.

I. INTRODUCTION

A major difficulty in understanding bonding in the solid state is the lack of an adequate set of electronic wave functions. The use of "free-ion" wave functions is justified only by the lack of anything better. An important step toward understanding the effects of covalency on 3d electronic wave functions has been made by Alperin who measured the neutron-scattering form factor for Ni^{2+} in solids.¹ His results show a significant contraction of the 3d(e)-spin-density distribution, with respect to the predictions from free-ion calculations, which is in contrast with the apparent expansion observed for Mn^{2+} ion in solids by Hastings, Elliott, and Corliss²; he suggests that the discrepancy is due to the outstanding difference in the spin configurations of the two ions, e.g., e_g^2 vs $t_{2g}^3 e_g^2$ unpaired spins.

Recently, Freeman and Ellis have reported the

results of fully variational unrestricted Hartree-Fock calculations for $(\text{MnF}_6)^{4-}$ clusters.³ These authors obtain results which resolve the above paradox. While the spin-density distribution of the two unpaired e_g electrons is contracted and that of the three unpaired t_{2g} electrons is expanded, the net effect is that of an expansion in comparison with the free-ion Mn^{2+} .³

These results support our phenomenological analysis of the Mössbauer isomeric shift (IS) and quadrupole splitting (QS) for the ferrous halides^{4,5} and series of related compounds.^{6,7} This analysis shows that a predominant effect of covalency in the high-spin octahedral ferrous compounds is the radial expansion of the 3d(t_{2g}) wave functions.

In the present work we analyze the Mössbauer hyperfine interactions of two series of octahedral, high-spin, and ionic, as well as intermediate ferrous compounds in terms of the radial distribution

of the $3d$ unpaired spin (or charge) densities. When the present analysis is extended to covalent low-spin octahedral iron compounds, it leads to a model in which charge densities are varying continuously on going from completely ionic to completely covalent compounds. Corroborative information will be derived from neutron scattering, EPR, optical spectroscopy, and studies in crystal structures.

II. HYPERFINE INTERACTIONS

The observed internal magnetic field at the nucleus may be described in terms of three components:

$$H_{\text{int}} = H_c + H_L + H_D, \quad (1)$$

where H_c is the Fermi contact interaction caused by the interaction of the nuclear magnetic moment with the spin-density distribution of the atomic s electrons at the nucleus, polarized via exchange interaction with the unpaired d electrons; H_L is the contribution from the orbital current due to the unquenched angular momentum, and H_D is the component due to the anisotropy of the spin-density distribution and should vanish for a strictly cubic ligand configuration. Equation (1) may be rewritten as⁸

$$H_{\text{int}} = H_c + 4\beta \langle r^{-3} \rangle \Omega_i, \quad (2)$$

where

$$\Omega_i = (g_i - 2) + \frac{1}{14} \langle 0 | L_i^2 - 2 | 0 \rangle,$$

and g_i and L_i are the components of the electron g factor and the angular momentum operator, respectively. While the second term in Eq. (2) depends linearly on $\langle r^{-3} \rangle$ of the single t_{2g} electron, the contribution of the contact term depends on both unpaired t_{2g} and e_g electrons. A partial cancellation of covalency effects, that is, e_g contraction and t_{2g} expansion, on the total $3d$ -spin-density distribution is expected in FeF_2 similar to that in $(\text{MnF}_6)^{4-}$. However, it is not clear *a priori* whether the net effect on H_c in FeF_2 would be that of contraction or expansion of the total-spin-density distribution with respect to that of the free ion.

Complementary information with regard to the expansion of the t_{2g} -charge-density distribution may be obtained from the quadrupole splitting, which may be written as

$$\Delta E = (\Delta E)_0 \alpha_c^2 F(\Delta_1, \Delta_2, \alpha_s^2 \lambda_0, T), \quad (3)$$

where $(\Delta E)_0$ is a normalization factor corresponding to the contribution from a single t_{2g} electron of a nondegenerate free-ion ground state; ΔE differs from $(\Delta E)_0$ by $\alpha_c^2 = \langle r^{-3} \rangle / \langle r^{-3} \rangle_{\text{ion}}$ and the function F , which represents the quenching due to the mixing of the t_{2g} levels, by the spin-orbit interaction as well as the effect of thermal population of higher t_{2g} levels. The reduction of the spin-

orbit coupling constant in the solid, with respect to the free-ion value, is represented by $\lambda = \alpha_s^2 \lambda_0$. In view of the introductory remarks, the covalency factor α_c^2 is expected to be larger than α_c^2 since the spin-orbit interaction reflects covalency effects on both t_{2g} and e_g unpaired spins, while α_c^2 describes the expansion of the single t_{2g} electron only.

The quenching of ΔE at very low temperatures by the spin-orbit interaction will depend on the ratio between λ and the crystal-field-splitting parameters Δ_1 and Δ_2 . For all practical purposes, this effect may be neglected as long as $\alpha_s^2 \lambda_0 \ll \Delta$. Detailed theoretical analysis of ΔE data for several cases yielded crystal field parameters which are significantly lower than those obtained at helium temperatures by other methods.⁹⁻¹¹ This indicates strong thermal variation of crystal field parameters.¹² If this is indeed the case, the usefulness of Eq. (3) is limited to the verification this effect. For the purpose of the present analysis, it is important to verify that crystal field splitting is large enough so that the quenching of ΔE by the spin-orbit interaction may be neglected at low temperatures. It has been shown in several circumstances that lattice contributions to ΔE may be neglected for compounds of moderately distorted octahedral symmetry. Consequently, if the thermal variation of ΔE is relatively small up to room temperature, which implies that the crystal field splitting Δ is significantly larger than the spin-orbit interaction, F would be considered as 1 for a singlet and $\frac{1}{2}$ for a doublet ground state. With this approximation, the low-temperature value of ΔE may be used to estimate $\langle r^{-3} \rangle$ of the single t_{2g} electron. Caution must be exercised in the case of degenerate ground states. Antiferromagnetic phase transitions are quite commonly accompanied by structural distortions^{13,14} which may remove the degeneracy of the electronic ground state at low temperatures. Wertheim *et al.* reported the observation at helium temperatures of $\Delta E \sim 2.7$ mm/sec for RbFeF_3 , which is of cubic symmetry at higher temperatures.¹⁵ This magnitude is very similar to the $\Delta E \sim 2.9$ mm/sec observed for FeF_2 which has a singlet ground state. It would suggest that the triplet degeneracy is completely removed by the structural distortion accompanying the antiferromagnetic transition in RbFeF_3 . This effect must be borne in mind in the discussion of the unusual thermal variation of ΔE in the low-temperature metamagnetic phases in the heavier ferrous halides (Fig. 1).

After taking the precautions discussed above, the low-temperature values of ΔE may be used to estimate $\langle r^{-3} \rangle$ for the t_{2g} -charge-density distribution. Then, assuming that this distribution is the same for the unpaired t_{2g} spin densities, it may be inserted into Eq. (2) for the analysis of H_{int} , while Ω_i has to be evaluated separately.

The third parameter which is associated with the electronic-charge-density distribution and derived from the Mössbauer spectra is the IS. The IS is due to the electrostatic interactions between the charge-density distributions of the nuclear levels, participating in the Mössbauer resonance, and the atomic electrons. Since only s electrons have finite probability to penetrate the volume occupied by the nucleus, their contribution to IS is dominant. Changes in covalency would directly affect IS via the increase in $4s$ participation in the bond, and indirectly, by the shielding of the s electrons by the $3d$ electrons. IS depends on the total-charge-density distribution and its interrelations with ΔE and H_{int} are not obvious. In contrast, ΔE depends mainly on the distribution of the single antibonding t_{2g} electron and H_{int} on the distribution of the unpaired spins. Ultimately, the investigation of the interrelation between those three experimental parameters may provide some insight into covalent bonding in solids.

III. NORMALIZATION OF $\langle r^{-3} \rangle$ SCALE

The problem of theoretical interpretation of QS and H_{int} data for a single compound involves too many unknown parameters and is therefore under-determined. It would be appropriate, therefore, to apply the analysis simultaneously to a series of

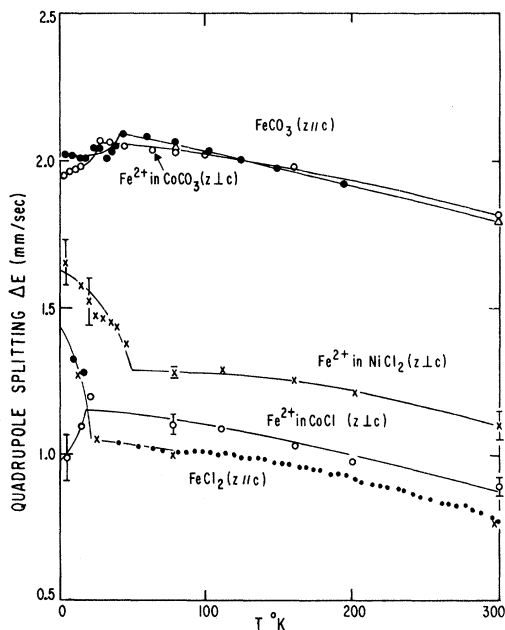


FIG. 1. ΔE data for some metamagnetic compounds. Data for FeCO_3 and CoCO_3 are reproduced from tabulated results in Refs. 19 and 25. Room-temperature point for FeCO_3 is taken from R. W. Grant *et al.* [*J. Chem. Phys.* **45**, 1015 (1966)]. Results for FeCl_2 , CoCl_2 , and NiCl_2 are from Refs. 5 and 23.

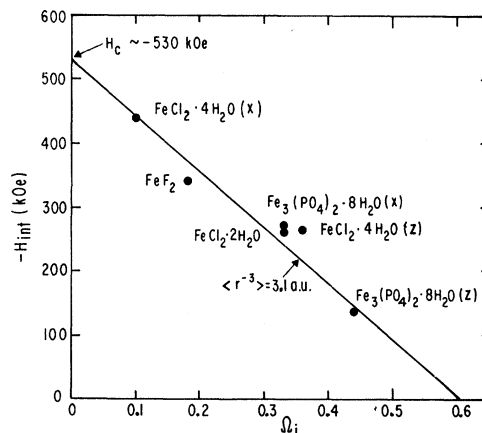


FIG. 2. H_{int} vs Ω_i for some Fe^{2+} compounds.

compounds. In our attempt to normalize the $\langle r^{-3} \rangle$ scale for the t_{2g} electron we will compare the H_{int} data for a group of compounds [$\text{FeCl}_2 \cdot 2\text{H}_2\text{O}$, FeF_2 , $\text{Fe}_3(\text{PO}_4)_2 \cdot 8\text{H}_2\text{O}$, and $\text{FeCl}_2 \cdot 4\text{H}_2\text{O}$]. These compounds have similar ΔE values at low temperatures (2.6, 2.9, 3.0, and 3.1 mm/sec, respectively) and would be expected to be associated with $\langle r^{-3} \rangle$ of similar magnitudes.

The analysis of H_{int} for these compounds in terms of Eq. (2) is shown in Fig. 2 and the relevant parameters are tabulated in Table I. These data have been first discussed by Johnson who observed the approximate linear relation between H_{int} and Ω_i . He observed that this is consistent with single values for $\langle r^{-3} \rangle$ as well as H_c for this group of compounds.⁸ In our previous discussions of the QS-IS correlations in the ferrous halides and their hydrates,⁴⁻⁷ we have assigned $\alpha_c^2 \sim 0.6$ for FeF_2 . This value, multiplied by the theoretical estimate of $\langle r^{-3} \rangle_{\text{ion}} = 5.1$ a. u., yields $\langle r^{-3} \rangle \sim 3.1$ a. u. for FeF_2 . In view of the similarity in the ΔE values observed for the above compounds (Table I), the straight line associated with the above value of $\langle r^{-3} \rangle$ is expected also to fit the H_{int} data, which is indeed the case (Fig. 2). The internal consistency between the QS-IS analysis and the results of the internal magnetic fields is reassuring. The good

TABLE I. Hyperfine data for some ferrous compounds. These data are taken from Ref. 8 and references therein; are the experimental values at low temperatures.

	ΔE (mm/sec)	i	H_i (kOe)	Ω_i
$\text{FeCl}_2 \cdot 4\text{H}_2\text{O}$	3.1	x	-440	0.10
		z	-266	0.36
$\text{Fe}_3(\text{PO}_4)_2 \cdot 8\text{H}_2\text{O}$	3.0	x	-270	(0.33)
		z	-135	(0.44)
FeF_2	2.9	x	-330	0.18
$\text{FeCl}_2 \cdot 2\text{H}_2\text{O}$	2.6	x	-260	0.33

agreement between the predictions of the two methods indicates that $\langle r^{-3} \rangle$ values measured by both of them are very closely the same. Consequently, one can use the predictions from QS data in the analysis of the H_{int} results.

The magnitude of the contact interaction term H_c is obtained from the intersection of the straight line in Fig. 2 with the $\Omega_i = 0$ ordinate. The value of $H_c = -530 \pm 40$ kOe so obtained is very close to the calculated one of -550 kOe for the Fe^{2+} free ion.¹⁶ This value is in conflict with the large radial expansion predicted from the slope of the straight line in Fig. 2. This paradox may be resolved in the same manner as the one between the neutron form factors for Mn^{2+} and Ni^{2+} in solids.² While the expanded spin-density distribution of the three t_{2g} electrons in Mn^{2+} more than compensates for the contraction of the two e_g electrons, the near cancellation of the two effects will explain the near-free-ion value of H_c in FeF_2 .

It will be instructive at this point to compare the present calibration of the $\langle r^{-3} \rangle$ scale with the results of the neutron-scattering form-factor measurements. Hastings *et al.* reconcile their experimental results with the free-ion calculations for Mn^{2+} ions by proposing a mean $3d$ radius in the respective solid compounds which is 10% larger than the free-ion value.² This amounts to a reduction of 0.73 in the mean spin density (per electron) of the $3d(t_{2g}^3 e_g^2)$ subshell in these compounds. Similarly, Alperin's results for NiO correspond to a large increase in the average $3d$ spin density, which consists of e_g electrons only.¹ In view of the opposing contributions from the t_{2g} and e_g electrons, the above average value of 0.73 represents an upper limit to the reduction factor for the mean spin density of a t_{2g} electron in Mn^{2+} ion. This observation supports, therefore, the covalency reduction factor of $\alpha_c^2 \sim 0.60$, assigned above to describe the t_{2g} -charge-density distribution in FeF_2 . For reference in the following discussions, let us recall that the value of $\alpha^2 \sim 0.60$ has been originally proposed to account for EPR data.¹⁷

IV. TRIGONALLY DISTORTED OCTAHEDRAL COMPOUNDS

In view of the consistency observed above between the predictions for $\langle r^{-3} \rangle$ of the t_{2g} electron, from ΔE and H_{int} analysis, it would be instructive to extend the comparison to the other members of the ferrous-halides series. This can be done using the data for the additional two compounds FeCO_3 ^{18,19} and FeTiO_3 ,²⁰ which are of the same symmetry of ligand configuration as FeCl_2 , FeBr_2 , and FeI_2 , and for which a detailed analysis has been published by Okiji and Kanamori.²¹ All five compounds are of trigonal symmetry with a doublet ground state²² and, with the exception of FeTiO_3 , are known to

undergo metamagnetic transitions at low temperatures.^{19,23,24} The metamagnetic transitions in FeCl_2 , FeBr_2 , and FeI_2 , as well as Fe^{2+} impurities in NiCl_2 , are associated with dramatic increases in ΔE below T_c .^{5,24} In contrast, ΔE decreases below T_c for FeCO_3 ¹⁹ as well as for Fe^{2+} impurities in CoCO_3 ²⁵ and CoCl_2 ²³ (Fig. 1). The interpretation of the behavior of ΔE below the metamagnetic transition temperatures is important in the QS-IS analysis for the present series of compounds. This may be seen from the controversy between our conclusions⁴⁻⁷ and those of Fugita, Ito, and Ono.²³ These authors explain the decrease of ΔE below T_c for Fe^{2+} impurities in CoCl_2 , as opposed to FeCl_2 , by assuming that the spins of the Fe^{2+} ions are parallel to the direction of magnetization in both cases. Consequently, the opposite behavior below T_N may be accounted for by the fact that the direction of magnetization is parallel to the c axis in FeCl_2 and perpendicular to it in CoCl_2 . Following this interpretation, it is necessary to assume that the spins of the Fe^{2+} impurities are parallel to the c axis in NiCl_2 and therefore perpendicular to the direction of magnetization in the host lattice. The direction of magnetization is known to be parallel to the crystallographic c axis for FeCO_3 ,¹⁹ and perpendicular for CoCO_3 ²⁵ and the decrease in ΔE below T_c in both cases is therefore unexplained. It appears that the understanding of the ΔE anomalies below T_c in this group of compounds awaits further investigation.

Inspection of the ΔE curves shown in Fig. 1 would suggest that, while the nature of the behavior below T_c is not yet understood, the behavior above the transition temperatures seems to better characterize the bonding with the corresponding ligands. In other words, apart from a magnitude factor, the ΔE curves for FeCO_3 are the same as that for Fe^{2+} impurities in CoCl_2 , and the latter is very similar to the ΔE curves for FeCl_2 and Fe^{2+} impurities in NiCl_2 , above T_c , while differing significantly from them below T_c .

The same symmetry of the Fe^{2+} sites in FeCO_3 , FeTiO_3 , FeCl_2 , FeBr_2 , and FeI_2 makes it appropriate to analyze their hyperfine interactions within the same theoretical framework. Consequently, we will apply the results of Okiji and Kanamori to all of them, using $\langle r^{-3} \rangle$ estimates obtained from the QS data. Because of the double degeneracy of the t_{2g} ground level, we will use $\Delta E' = 2\Delta E$ (above the corresponding metamagnetic transitions). This is essentially an identical approach to the one used in our previous work.⁴⁻⁷ We are using here, however, newly available data, reproduced in Fig. 1, to further support this point of view.

To test this approach we will estimate $\langle r^{-3} \rangle$ for FeCO_3 by comparing it to FeF_2 . Using $\Delta E' = 4.2$ mm/sec for FeCO_3 and $\Delta E = 2.9$ mm/sec and $\langle r^{-3} \rangle$

= 3.1 a. u. for FeF_2 , the estimate would be $\langle r^{-3} \rangle \cong 4.4$ a. u. for FeCO_3 . This is the same value as used by Okiji and Kanomori in their analysis.²² These authors interpolated between values deduced by Abraham, Horowitz, and Pryce for V^{2+} , Mn^{2+} , Co^{2+} , and Cu^{2+} from EPR data.²⁶ The value of $\langle r^{-3} \rangle = 4.4$ a. u. is significantly smaller than the free-ion value of 5.1 a. u., proposed by Watson and Freeman.¹⁶ Assuming that the difference includes both effects of radial expansion and molecular-orbital-type mixing with ligand orbitals, and using $\langle r^{-3} \rangle = 4.4$ a. u., the second term in Eq. (2) may be estimated for FeCO_3 as $H_L + H_D \sim +730$ kOe.²⁷ Comparing with the experimental value of $H_{\text{int}} = +184$ kOe^{18,19} one obtains $H_c \sim -545$ kOe for FeCO_3 . The same analysis is carried out for the heavier halides and FeTiO_3 , using Eq. (2) and $\langle r^{-3} \rangle$ values derived from the QS data. The results are tabulated in Table II and displayed in Fig. 3 as a function of $\langle r^{-3} \rangle$.²⁸

V. RELATION BETWEEN QS AND H_c

From the relation between H_c and QS, as displayed in Fig. 3, it appears that for the heavier halides the effect of the radial expansion of the t_{2g} dominates over the radial changes in the e_g wave functions. In the more ionic compounds, like FeF_2 , the attraction, between the Fe^{2+} ion and its relatively small ligands, is balanced by the compression of the electronic cloud along the bond directions. Such a compression in the bond directions may account for the apparent contraction observed in NiO for the $3d(e_g)$ wave functions.¹ Because of the increase of the ionic radii of the ligands in FeCl_2 , FeBr_2 , and FeI_2 the crystal structure is that of a close-packed arrangement of the ligands, with the Fe^{2+} ions occupying a sublattice of interstitial positions. The attraction between the Fe^{2+} ions and the ligands is balanced to a large extent by the overlap interaction between the ligands in the close-packed lattice. This increase in anion-anion repulsion reduces the compression of the charge density along the cation-anion bond direction. The increase of the size of the interstitials occupied by the Fe^{2+} ions reduces the contraction of the e_g charge density as well as provides room for the expansion of the t_{2g} wave functions.

TABLE II. Hyperfine data for some ferrous compounds.

	ΔE (mm/sec) (T_z, T_x)	$\Delta E' = 2\Delta E$ (mm/sec)	$\langle r^{-3} \rangle$ (a. u.)	H_{int} (kOe)	$H_L + H_D$ (kOe)	H_c (kOe)
FeCO_3	2.1 ^a	4.2	4.4	+184 ^a	+730 ^b	-546
FeTiO_3	1.14 ^c	2.28	2.4	-70 ^c	+400	-470
FeCl_2	1.03 ^d	2.06	2.15 + 3 ^e	+358	+358	-355
FeBr_2	0.86 ^d	1.72	1.8 + 30 ^e	+300	+300	-270
FeI_2	0.81 ^d	1.62	1.7 + 74 ^e	+280	+280	-206

^aReferences 18 and 19.

^bReference 27.

^cReference 20.

^dReference 4.

^eReference 24.

The net effect is that of expansion of the total-spin-density distribution. The observed decrease in magnitude of H_c is consistent with the theoretical results of Watson and Freeman.¹⁶ These authors predicted a decrease in magnitude, with an eventual change of sign of H_c , as a result of significant radial expansion of the 3d wave functions.

Within the framework of the present interpretation of the H_c -QS relationship, in the octahedral high-spin ferrous compounds, one may predict by extrapolation that any further increase in covalency would result in a positive value for H_c . An appropriate compound for an extension of the present analysis is FeS. It is of the NiAs structure, and the Fe^{2+} ion may be expected to be subjected to a trigonal distortion from strict octahedral symmetry. In fact, the situation is more complicated and the point-group symmetry is lower than trigonal.^{29,30} A comparison of the QS-IS values of FeS with those for the compounds discussed above (Fig. 4) supports such an extension. Because of the rather small $\langle r^{-3} \rangle$ indicated by the small value of $\Delta E \sim 0.9$ mm/sec, the correction due to the second term in Eq. (2) is expected to be small. The removal of the double degeneracy due to the distortion from trigonal symmetry would further reduce the contribution from this term. The correction due to $H_L + H_D$ is estimated as $+100 \pm 50$ kOe. Depending on the sign, the measured value of $|H_{\text{int}}| = 309$ kOe³⁰ corresponds to H_c values of $+210 \pm 50$ or -410 ± 50 kOe. The present analysis (Fig. 3) favors $H_c \sim +210 \pm 50$ kOe for FeS and, consequently, the positive sign for H_{int} . The sign of H_{int} has not been determined experimentally.

VI. EXTENSION TO COVALENT COMPOUNDS: FeS_2

In an attempt to explore the implications of the present results to the understanding of covalency, in general, in ferrous compounds, the analysis has been extended to include the covalent compound FeS_2 .

The purpose of including FeS in the analysis is to provide a bridging case between the "ionic" and "covalent" iron compounds. A major aspect of covalency in FeS_2 is its being of the low-spin configuration t_{2g}^6 . Consequently, the observed ΔE in this compound is due to the strong crystalline distortion rather than a single t_{2g} electron. However, the contribution of a single t_{2g} electron to ΔE may be estimated by comparison of FeS_2 with FeSAs and FeAs_2 . These three isostructural compounds have the electronic configurations of t_{2g}^6, t_{2g}^5 , and t_{2g}^4 ³¹ and the low-temperature ΔE values of 0.61, 1.07, and 1.70 mm/sec, respectively.³² If the differences in ΔE are attributed to the removal of one and two (paired) t_{2g} electrons, consecutively, the contribution of each of them to ΔE would be ~ 0.55 mm/sec. This estimate is very close to the

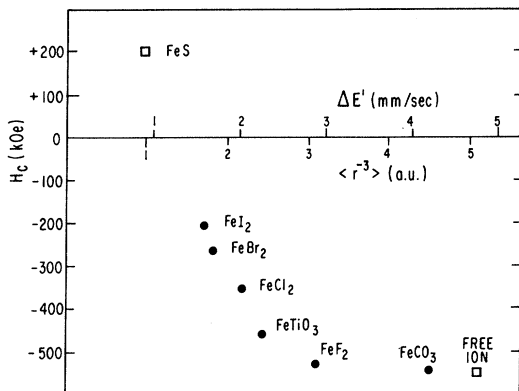


FIG. 3. H_c vs $\Delta E'$ for some ferrous compounds. $\Delta E'$ is the low-temperature value of ΔE for FeF_2 and FeS and is twice the ΔE value above the metamagnetic transition for all the other compounds. The point for FeF_2 is used for normalization of $\langle r^{-3} \rangle$ for the t_{2g} -charge-density distribution.

results observed for covalent ferric compounds such as $\text{Fe}^{\text{III}}\text{N}$, N -dialkyldithiocarbamates³³ and the ferricyanides.³⁴ These compounds have t_{2g}^5 electronic configurations and ΔE values which correspond to a missing t_{2g} electron, and which, insofar as the ΔE results are concerned, is equivalent to a single t_{2g} electron. With this value for ΔE , the QS-IS data for the low-spin compound FeS_2 are compared in Fig. 4 with the results for the high-spin compounds discussed above. It is significant that both QS and IS vary continuously, and almost linearly, with covalency on going from FeF_2 through the heavier halides and FeS to FeS_2 . The notion of continuous variation of charge densities with increasing covalency has been previously discussed by Erickson on the basis of IS data³⁵ and is further supported in the present work by the analysis of the QS and H_{int} results.

An important aspect of the covalency in FeS_2 is the large crystalline radius for the Fe^{II} ion in this compound. The crystalline radii are derived from the analysis of crystal structures and the value assigned by Pauling for Fe^{II} in FeS_2 is 1.23 Å.³⁶ The crystalline radius of Fe^{2+} in FeF_2 may be derived in a similar manner by subtracting the ionic radius of F^- (1.36 Å)³⁶ from the average Fe-F distance (2.08 Å).³⁷ The value so obtained for the Fe^{2+} ion in FeF_2 is 0.72 Å. The ratio between the volumes, occupied by Fe^{II} in FeS_2 and by Fe^{2+} in FeF_2 , is given approximately by the third power of the ratio between the corresponding crystalline radii, which is $(1.23/0.72)^3 = 5$. This result is similar to the ratio of ~ 5.3 between the corresponding ΔE and therefore the $\langle r^{-3} \rangle$ values. This similarity implies that $\langle r^{-3} \rangle$ varies approximately like $\langle r \rangle^{-3}$ of the $3d$ charge distribution. Consequently, the variation in the $3d(t_{2g})$ wave function

may be represented to a good approximation by a radial scaling factor.

$$\psi_{3d}(\text{solid}) = \psi_{3d}^{\text{ion}}(\beta_0 r, \theta, \phi), \quad (4)$$

where the scaling factor β_0 has been related by Jørgensen to an effective charge on the metal ion. This effective charge is associated with the increase in covalency and reflected in the nephelauxetic effect.³⁸ In a simple approximation, the outermost $3d$ electron may be described by a hydrogenlike wave function, with the nuclear charge and all other electrons considered to be at the center³⁶

$$R_{3d}(r) \propto (2Z^*r/3a_0)^2 e^{-2Z^*r/3a_0}. \quad (5)$$

In this approximation, Z^* would be 1 for the neutral iron atom and 3 for the Fe^{2+} free ion. Changes of the central effective charge due to covalency would be described by $1 \leq Z^* \leq 3$. These variations may be described by $\beta_0 = Z^*/Z$ (with $Z = 3$ in the present case), where $\frac{1}{3} \leq \beta_0 \leq 1$ and the limits $\frac{1}{3}$ and 1 correspond to the completely covalent and completely ionic cases, respectively. Within this approximation

$$\alpha_c^2 = \langle r^{-3} \rangle / \langle r^{-3} \rangle_{\text{ion}} = (\langle r^{-1} \rangle / \langle r^{-1} \rangle_{\text{ion}})^3 = \beta_0^3. \quad (6)$$

The correctness of this expression depends, of course, on the validity of the assumption that covalency effects are represented, to a good approximation, by the radial scaling factor β_0 . This assumption was based above on the relation between the experimental ΔE values and the empirical crystalline radii. It implies $\frac{1}{27} \leq \alpha_c^2 \leq 1$, allowing for a large range of variation of $\langle r^{-3} \rangle$ in solids. An

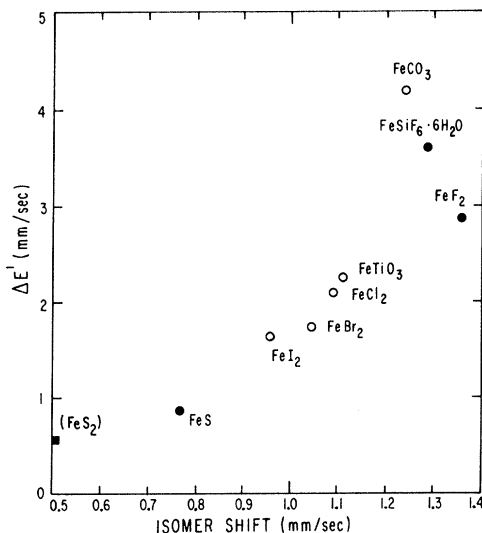


FIG. 4. $\Delta E'$ vs IS for some iron compounds. IS values vs metallic iron at room temperature. The open circles are for $\Delta E' = 2\Delta E$ and the enclosed circles are for $\Delta E' = \Delta E$, as explained in the text. The data point for FeS_2 is discussed in the text.

alternative, and most commonly used, way to describe the reduction of $\langle r^{-3} \rangle$ in solids is through the formalism of molecular-orbital (MO) theory. Within this formalism, the variation of $\langle r^{-3} \rangle$ is limited by $\frac{1}{2} \leq \alpha_{\text{MO}}^2 \leq 1$.³⁹ The fact that much smaller values are observed for α_c^2 emphasizes the importance of the radial expansion.⁶ In order to account for both radial expansion and MO mixing, Eq. (6) may be rewritten as

$$\alpha_c^2 = \beta_0^3 \alpha_{\text{MO}}^2 \quad (7)$$

The dominance of the radial expansion in the case of FeS₂ is supported by the results of optical spectroscopy. The interelectronic repulsion parameter B , derived from the optical spectra, is caused by the Coulombic repulsion and is related to $\langle r^{-1} \rangle$ and, therefore, to β_0 . The estimate available from optical spectroscopy, for a Fe^{III} ion surrounded by six sulfur ligands, is $\beta = 0.47$.⁴⁰ Using the $\langle r^{-3} \rangle$ scale shown in Fig. 3, one can deduce a value of $\alpha_c^2 = 0.115$ from the ΔE associated with the removal of one t_{2g} electron from FeS₂. Assuming that the effect of MO mixing is rather small, and using, therefore, Eq. (6), this value of α_c^2 corresponds to $\beta_0 = 0.48$, which is in excellent agreement with the above estimate available from optical spectroscopy. In view of the large uncertainties involved in these estimates, it is reassuring that similar ΔE and β values are also obtained for the covalent complexes of iron cyanides.^{34,38}

The effective charge Z^* , described above, differs from the commonly used concept of effective ionic charge by the unity charge of the outermost 3d electron. Consequently, the result of $\beta_0 \approx 0.48$ corresponds to $Z^* \approx +1.4$, or to an effective ionic charge of $Z^* - 1 \approx +0.4$ for the covalent compound FeS₂. Effective ionic charges have quantitative meaning only within the context of the theoretical expression from which they are derived, which in the present case is Eq. (5). It is reassuring, however, that the low value of +0.4 is in a qualitative good agreement with the generally accepted notions of covalency.

VII. SUMMARY AND CONCLUSIONS

The main purpose of the present work is to present a model which describes the variation of the 3d-charge-density distribution with covalency. This model applies to the ionic, covalent, as well as intermediate ferrous compounds with approximately octahedral symmetry. Some insight into covalency in the complete ionic end is obtained from neutron-scattering form-factor data. Important aspects of covalency at the covalent end may be derived from the examination of the empirical crystalline radii.

Analysis of the Mössbauer hyperfine interactions leads to a model which ties up the two ends together. The interpretation of the Mössbauer results supports the observation, from neutron-scattering form-factor experiments, that for moderate degree of covalency, the dominant effects are those of radial t_{2g} expansion accompanied by e_g contraction. The two opposing effects cancel each other up to a certain degree of covalency, insofar as the magnetic contact interaction is concerned. For higher covalency the expansion effect dominates. The radial 3d wave function changes continuously with covalency on going from the ionic, through the intermediate, to the covalent compounds. This variation results in a factor of ~ 10 change in the mean 3d charge density between the two extremes. These observations are consistent with a change of about a factor of 2 in the observed crystalline radii, as well as similar changes observed in the interelectronic repulsion term B , derived from optical spectroscopy. The $\langle r^{-3} \rangle$ scale derived in the present work compares well at two different cases, FeF₂ and FeCo₃, with the predictions from EPR results. It is also consistent with the theoretical estimate by Watson and Freeman of $\langle r^{-3} \rangle \approx 5.1$ a. u. for the Fe²⁺ free-ion 3d wave functions. The present work suggests a $\langle r^{-3} \rangle$ value of ~ 0.5 a. u. for the t_{2g} electrons in covalent compounds. If the effective ionic charge on the covalent iron atom is believed to be negligibly small, this value would correspond to the free-atom 3d wave function. The large variation in $\langle r^{-3} \rangle$, on going from the completely ionic to the completely covalent compounds, may be anticipated from the intimate relation between the radial expansion and the effective charge, as is illustrated by Eq. (5).

A large range of radial modifications of the 3d electronic wave functions in octahedral ferrous compounds has been demonstrated in the present work. These modifications cannot be accounted for by theoretical bonding models, such as crystal field and MO theories, which are based on the free-ion wave functions. These results support the recent approach, by Freeman and Ellis, in which self-consistent-field-type computations are carried out with the radial wave functions described by variational rather than fixed parameters.

ACKNOWLEDGMENTS

Work supported by the U. S. Atomic Energy Commission. The author expresses his appreciation to Professors N. Benczer-Koller and R. H. Herber for critical reading of the manuscript.

¹H. A. Alperin, Phys. Rev. Letters **6**, 55 (1961).

²J. M. Hastings, N. Elliott, and L. M. Corliss, Phys.

Rev. **115**, 13 (1959).

³A. J. Freeman and D. E. Ellis, Phys. Rev. Letters

24, 516 (1970).

⁴R. C. Axtmann, Y. Hazony, and J. W. Hurley, Jr., *Chem. Phys. Letters* 2, 673 (1968).

⁵Y. Hazony and H. N. Ok, *Phys. Rev.* 188, 591 (1969).

⁶Y. Hazony, R. C. Axtmann, and J. W. Hurley, Jr., *Chem. Phys. Letters* 2, 440 (1968).

⁷R. C. Axtmann, Y. Hazony, and J. W. Hurley, Jr., *J. Chem. Phys.* 52, 3309 (1970).

⁸C. E. Johnson, *Symp. Faraday Soc.* 1, 7 (1967).

⁹R. Ingalls, *Phys. Rev.* 133, A787 (1964).

¹⁰R. Ingalls, K. Ono, and L. Chandler, *Phys. Rev.* 172, 295 (1968).

¹¹U. Ganiel and S. Shtrikman, *Phys. Rev.* 177, 503 (1969).

¹²Y. Hazony, *Discussions Faraday Soc.* 48, 148 (1969).

¹³A. Okazaki and Y. Suemune, *J. Phys. Soc. Japan* 16, 671 (1961).

¹⁴J. W. Philip, R. Gonano, and E. D. Adams, *Phys. Rev.* 188, 973 (1969).

¹⁵G. K. Wertheim, H. J. Guggenheim, H. J. Williams, and D. N. E. Buchanan, *J. Appl. Phys.* 39, 1253 (1968).

¹⁶R. E. Watson and A. J. Freeman, *Phys. Rev.* 123, 2027 (1961).

¹⁷M. Tinkham, *Proc. Roy. Soc. (London)* A236, 549 (1956).

¹⁸D. W. Forester and N. C. Koon, *J. Appl. Phys.* 40, 1316 (1969).

¹⁹H. N. Ok, *Phys. Rev.* 185, 472 (1969).

²⁰G. Shirane and S. L. Ruby, *J. Phys. Soc. Japan* 17, 133 (1962).

²¹A. Okiji and J. Kanamori, *J. Phys. Soc. Japan* 19, 908 (1964).

²²J. Kanamori, *Progr. Theoret. Phys. (Kyoto)* 20, 890 (1958).

²³T. Fugita, A. Ito, and K. Ono, *J. Phys. Soc. Japan* 27, 1143 (1969).

²⁴D. J. Simkin, *Phys. Rev.* 177, 1008 (1969).

²⁵H. N. Ok, *Phys. Rev.* 181, 563 (1969).

²⁶A. Abragam, J. Horowitz, and M. H. L. Pryce, *Proc. Roy. Soc. (London)* A230, 169 (1955).

²⁷The difference between the present estimate of $H_L + H_D = +730$ kOe and the value of $+670$ kOe given in Ref. 21 for FeCO_3 is due to an additional covalency reduction factor, of about 0.9, which has been arbitrarily assumed by Okiji and Kanamori. This additional correction factor is not used in the present analysis and all covalency effects are assumed to be accounted for by the reduced values of $\langle r^{-3} \rangle$ (with respect to the free-iron value of 5.1 a.u.) given in column 4, Table II.

²⁸An additional compound of trigonal symmetry, not shown in Fig. 3 and for which an analysis of the hyper-

fine interactions is available, is ferrous fluosilicate [Johnson, *Proc. Phys. Soc. (London)* 92, 748 (1967)]. The crystal field at the Fe^{2+} site in ferrous fluosilicate is of trigonal distortion from octahedral symmetry, with a singlet rather than a doublet t_{2g} ground state. The Mössbauer spectra of ferrous fluosilicate have been measured at low temperatures by Johnson in external magnetic fields of up to 30 kOe. Only a small hyperfine field, ~ 14 kOe at 4.2°K, was observed for the external field H parallel to the trigonal axis of the crystal (for which the susceptibility is small). For H along any axis x in the plane perpendicular to z , a large effective field, ~ 100 kOe, was observed. From these values, the author extrapolates $H_{\text{int}}(z) = -550$ kOe and $H_{\text{int}}(x) = -248$ kOe. The comparison between the two yields $\langle r^{-3} \rangle \sim 3.5$ a.u. and $H_c \sim -420$ kOe. The author points out, however, that these results depend upon the measurements of small internal fields at the nucleus and rely upon the values of magnetization in 30 kOe, calculated from a spin Hamiltonian deduced from low-field susceptibility data. With this reservation in mind, those results may be considered as in good agreement with the predictions of the present analysis, which would be $\langle r^{-3} \rangle \sim 3.8$ a.u. (from the observed low-temperature value of $\Delta E \sim 3.6$ mm/sec) and $H_c \sim -540$ kOe (interpolation between the results for FeCO_3 and FeF_2 , Fig. 3). The present predictions would be $H_{\text{int}}(z) \sim -680$ kOe and $H_{\text{int}}(x) \sim -350$ kOe, which are not inconsistent with Johnson's extrapolated estimates.

²⁹S. S. Hafner, B. J. Evans, and G. M. Kalvius, *Solid State Commun.* 5, 17 (1967).

³⁰S. Hafner and M. Kalvius, *Z. Krist.* 123, 443 (1966).

³¹F. Hulliger and E. Mooser, *J. Phys. Chem. Solids* 26, 429 (1965).

³²P. Imbert, A. Gerard, and M. Winterberger, *Compt. Rend.* 256, 4391 (1963).

³³R. Rickards, C. E. Johnson, and H. A. O. Hill, *J. Chem. Phys.* 48, 5231 (1968).

³⁴W. T. Oosterhuis and L. G. Lang, *Phys. Rev.* 178, 439 (1969).

³⁵N. E. Erickson, *The Mössbauer Effect and its Application in Chemistry* (American Chemical Society, Washington, D. C., 1967).

³⁶L. Pauling, *The Nature of the Chemical Bond*, 3rd ed. (Cornell U. P., Ithaca, N. Y., 1960), p. 248.

³⁷J. W. Stout and R. G. Shulman, *Phys. Rev.* 118, 1136 (1960).

³⁸C. K. Jørgensen, *Oxidation Numbers and Oxidation States* (Springer-Verlag, New York, 1969).

³⁹J. Owen, *Proc. Roy. Soc. (London)* A227, 183 (1955).

⁴⁰A. H. Ewald, R. L. Martin, I. G. Ross, and A. H. White, *Proc. Roy. Soc. (London)* A280, 235 (1964).